CDF note 7929

Identification Efficiencies for Photons from Heavy, Long-Lived, Neutral Particles

Max Goncharov, David Toback, and Peter Wagner
Texas A&M University
(Dated: May 14, 2006)

Photons from heavy particles with nanosecond lifetimes can have a very displaced vertex and are usually not emitted in the flight direction of the decay parent. This causes the incident angle at the face of the electromagnetic calorimeter to be large compared to that from prompt photons from the primary interaction point. For this case we review the ID efficiencies for central ($|\eta| < 1$) photons as a function of incident angle using *cdfSim*. We conclude that all variables, except the CES-χ^2, are well modeled and retain roughly the same efficiency at large angles, so that they can be used unchanged to identify photons.

I. INTRODUCTION

The installation of the EMTiming system [1] was completed in Fall 2004 and commissioned in early 2005. It allows for a measurement of the arrival time of electromagnetic particles in the electromagnetic (EM) calorimeter with a resolution of under 1 ns [2]. In particular it is possible to select photons that have an arrival time incompatible with the time of the primary interaction [3]. An example for this is a photon decaying from a heavy, long-lived neutralino as in GMSB models [4]. In this case the photon is emitted homogeneously at a decay vertex that can be many centimeters away from the primary interaction point, causing the incident angle at the face of the EM calorimeter to be large compared to prompt photons from the primary interaction vertex. We present a Monte Carlo (MC) study of the distributions of the ID variables of photons from long-lived, neutral particles and determine their efficiency for the standard central photon cuts [5]. The ID variables used to select photons are [6]:

(1) E_T

(2) CES X and Z fiducial

(3) Had/Em

(4) Cone 0.4 calorimeter energy isolation

(5) CES-χ^2 strips and wires

(6) Number of tracks

(7) Track p_T

(8) Cone 0.4 track isolation

(9) 2nd CES cluster $E \cdot \sin(\theta)$ (strip and wire E individually)

In the following we will call variables 3 through 8 photon ID variables, as the E_T is a kinematic requirement which we choose to be greater than 30 GeV, and requirement 2 is a fiducial cut. We treat the CES-χ^2 separately from the other photon ID variables because (a) this variable is most affected by large incident angles and (b) we use a more sophisticated Monte Carlo simulation of the photon shower in the calorimeter, "Geant 3 Wedge Simulation," (G3WS) [7] as the standard *cdfSim* simulation [8] only parameterizes the shower shape at the CES using test beam data and hence does not correctly take into account its variation with incident angle. We show that the efficiency of all photon ID cuts except the CES-χ^2 are roughly flat as a function of incident angle. Since the low angles CES-χ^2 efficiency from G3WS does not match the efficiency from *cdfSim* and since G3WS shows that the efficiency drops off at high incident angles, we give recommendations for users on how to proceed depending on their analysis type. After briefly describing in Section II the datasets that are used in this note, we show in Section III the incident angle distribution for photons from GMSB neutralinos and compare it to prompt, Standard Model (SM)-like photons in MC using *cdfSim*. In Section IV we plot the distributions of the central photon ID variables except the CES-χ^2 using cdfSim and study the efficiencies as a function of the incident angles in MC by comparing them to data using CEM electrons from $W \rightarrow e\nu$. The CES-χ^2 is treated in Section V. Finally, in Section VI we give options how to proceed with the CES-χ^2 requirement and conclude in Section VII.

II. DATASETS

Here we summarize the data samples that are used in this note to study the ID variables in the MCs and compare them to real data. Unless otherwise noted, all MC samples are generated with PYTHIA v.6.216 and simulated with *cdfSim* of cdfsoft release 6.1.2 [8]:

(1) We simulate photons from long-lived particles using a MC sample of GMSB SUSY events with parameters set according to the Snowmass Slope 8 such that the neutralino mass is $m_\chi = 110$ GeV and the lifetime $\tau_\chi = 10$ ns [9, 12]. We select the highest E_T photon that has a neutralino as a parent with the ID requirements shown in Table III. Figure 1 shows that an E_T cut of 30 GeV is reasonable. In order not to bias the photon ID variables by the rest of the event we do not consider events with a jet within $R = 0.7$ of the photon.

(2) Prompt photons are simulated using a MC sample with exactly the same settings as above, but with $\tau_\chi = 0$ ns.

(3) We compare the MC results to a data sample of central electrons from $W \to e\nu$ with run numbers 191208-196902 (145.7 pb^{-1}). We use the W_NOTRACK trigger and select events with at least one electron that fulfills the requirements shown in Table I.

(4) We verify the data results using a MC sample of central electrons from $W \to e\nu$ that pass the same requirements as the data sample above.

CEM Electron
$E_T > 30$ GeV
Fiducial: $\lvert X_{\mathrm{CES}}\rvert < 21$ cm && 9 cm $< \lvert Z_{\mathrm{CES}}\rvert < 230$ cm
$p_T > 50$ GeV or $0.9 < E/p < 1.1$
Track quality: 3x3SLx5 hits
No additional tracks from conversions and tridents
Global Event Cuts
$\not{E}_T$>30 GeV
exactly 1 vertex with $N_{\mathrm{trks}} \geq 4$ and $\lvert z\rvert < 60$ cm
transverse mass: $50 < m_T < 120$ GeV

TABLE I: The sample requirements to select electrons from $W \to e\nu$ events. We use topological and global event cuts in combination with loose calorimetry but tight track quality requirements. These produce a sample that contains electrons with (1) high enough purity but (2) a low bias for calculating the efficiency of photon cuts vs. incident angles. The track requirements for the vertex reconstruction [10] are listed in Table II.

Requirement
$p_T > 0.3$ GeV
$p_T > 1.4$ GeV $\vert\vert$ $\frac{dE}{dx} < 20$
$\lvert z_0\rvert < 120$ cm
$\mathrm{Err}(z_0) < 1$ cm
$\lvert\eta\rvert < 1.6$
NCotStSeg(5)$\geq$2
NCotAxSeg(5)$\geq$2
$\lvert t_0\rvert < 40$ ns
$0.05 < \mathrm{Err}(t_0) < 0.8$ ns

TABLE II: Track requirements for the vertex reconstruction.

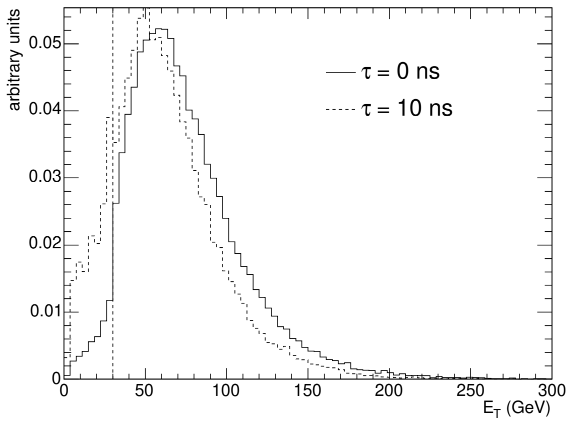

FIG. 1: The E_T distributions of photons from neutralinos with mass $m_\chi = 110$ GeV and lifetimes $\tau_\chi = 0$ (solid) and 10 ns (dashed). The dashed line indicates a cut at 30 GeV. This requirement is expected for future analyses [11], and is applied throughout the document.

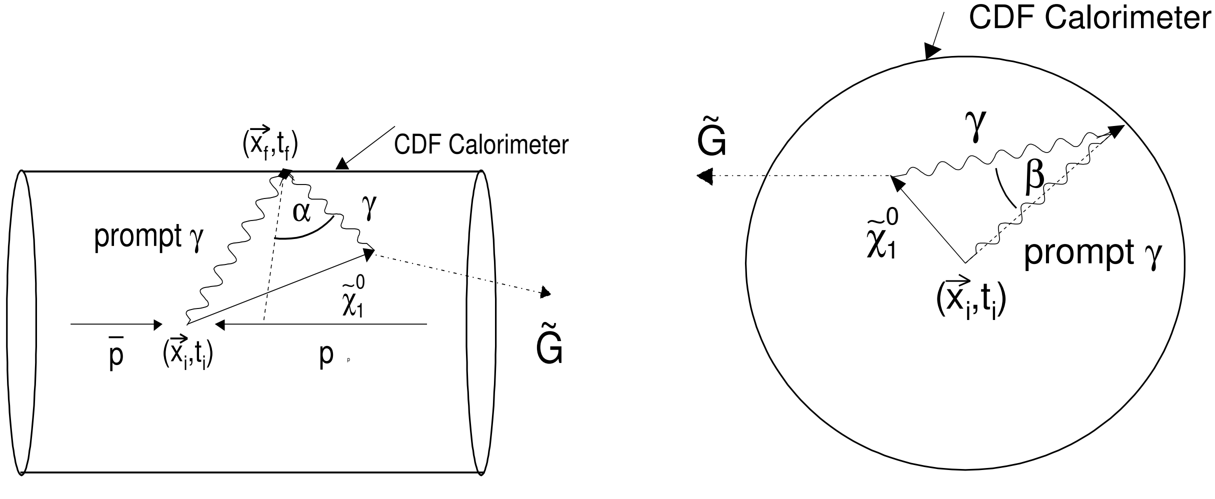

(a) (b)

FIG. 2: The definitions of the α and β incident angles using schematic diagrams of a long-lived neutralino decaying to a photon and a gravitino in the CDF detector in the (r,z)- and the (r,ϕ)-plane. The neutralino emanates from the collision at $(\vec{x}_i, t_i)$ and after a time τ it decays. While the gravitino leaves the detector the photon travels to the detector wall and deposits energy in the EM calorimeter where its final location $\vec{x}_f$ and arrival time t_f can be measured. A prompt photon would travel directly from $\vec{x}_i$ to $\vec{x}_f$. As the calorimeter towers point to the center of the detector we measure the incident angle of the photon with respect to the dashed line that extends from the calorimeter tower where the photon hits, to the center of the detector; α and β are the incident angles at the front face of the calorimeter in the (r,z)- and the (r,ϕ)-plane respectively. The CES shower in strips direction is affected by changes in α, the shower in the wires direction by changes in β. Note that for prompt production α can vary, but β is always 0.

III. INCIDENT ANGLE DISTRIBUTION OF PHOTONS FROM HEAVY, LONG-LIVED PARTICLES

We define the incident angle as the angle between the momentum vector of the photon and the momentum vector a prompt photon would have if it came from the center of the detector, arriving at the same location at the front face of the calorimeter, as shown in Fig. 2. The projection of the incident angle onto the (r, ϕ)-plane we call β, its projection onto the (r, z)-plane α, where z is the axis along the beam pipe. We make this distinction because, as shown later in detail, a change in α affects the ID efficiency of the CES strips subdetector (the strips run in the ϕ direction), while a change in β affects the efficiency in the wires subdetector (the wires run in the z direction). Figure 3 compares the incident angle distribution for prompt, SM like photons, simulated as decay products of neutralinos with $\tau_\chi = 0$ ns to photons from neutralinos with $\tau_\chi = 10$ ns. Also shown is the distribution for a photon after a requirement on the corrected arrival time [12], measured with the EMTiming system, of $2 < t_{\rm corr} < 10$ ns [13]. The prompt distributions have a maximum at 0° and extend to ∼18° in α while β is 0 as the beamline has negligible extent in the x-y plane. The incident angle α varies with the vertex z position of up to $|z| = 60$ cm. As the towers point to the center of the detector the angle extends out to $\sim 18^\circ \approx \arctan(60\text{cm}/183\text{cm})$ where 183 cm is the radius to the CES. The maximum of the GMSB distribution with 10 ns neutralino lifetime is at around 10°, extending out to maximum angles of ∼60° and ∼40° in α and β respectively with a large fraction of photons arriving at angles between 0 and 40° total incident angle. The distribution is largely independent of m_χ and τ_χ (tested for m_χ between 90 and 150 GeV and τ_χ between 10 and 35 ns). The timing requirement pushes the distribution out to higher incident angles with a maximum at ∼25°. As the incident angles of photons from long-lived particles are much larger than for prompt photons we will study if this affects the ID efficiency. Next we will present the distributions and efficiencies of all ID variables and then treat CES-χ^2 separately in Section V.

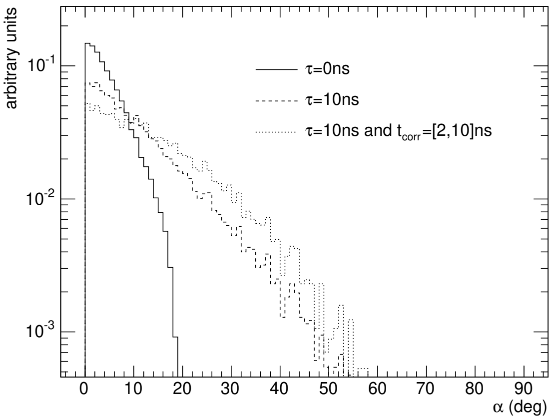

(a)

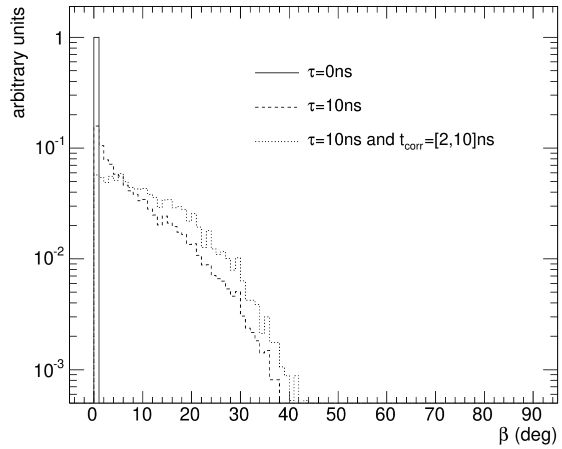

(b)

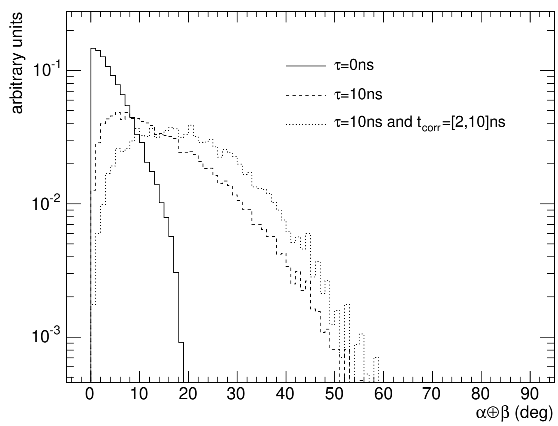

(c)

FIG. 3: The distribution of the incident angles α and β and the total incident angle $\alpha \oplus \beta$ at the front face of the central calorimeter for photons from neutralinos in a GMSB model (neutralino mass 110 GeV), simulated with *cdfSim*. We compare between "prompt" photons from neutralinos with 0 ns lifetime (solid) and a 10 ns lifetime (dashed). The dotted histogram shows the distribution for a lifetime of 10 ns for photons with an EMTiming corrected time between 2 and 10 ns. For α, while prompt photons have incident angles up to 20° with a maximum at 0° the distribution for photons from long-lived neutralinos extends out to 60°, with a large fraction between 0° and 40°. For β the angle is always zero for prompt production, but can extend to 40° in the long-lived case.

IV. PHOTON ID VARIABLE DISTRIBUTIONS AND EFFICIENCIES AS A FUNCTION OF α AND β USING *CDFSIM*

We next study the photon ID variable distributions and their efficiencies as a function of α and β. Figure 4 shows the distributions of the photon ID variables using the MC GMSB samples with a neutralino mass of 110 GeV produced with *cdfSim*. A comparison of photons from neutralinos with a lifetime of 0 ns to photons from neutralinos with a lifetime of 10 ns shows that the differences are, on average, very small. Table III summarizes the cumulative efficiencies ($N_{\text{pass this cut and all previous}}/N_{\text{pass fiducial}}$) and relative efficiencies ($N_{\text{pass this cut and all previous}}/N_{\text{pass all previous cuts}}$). The ID cuts are $\sim$1.5% less efficient for a lifetime of 10 ns than for prompt, dominated by the difference in the isolation distribution.

Figures 5, 6 and 7 show the relative efficiency of each ID variable as a function of incident angles α and β along with the results from our electron sample [14]. The efficiencies at low incident angles are similar for electrons from the W data sample and the MC photons from long-lived particles for all ID variables. Above that all ID variables are roughly flat as a function of α and β, except the energy isolation which falls slightly in β from $\sim$98% to $\sim$90% at 50° accounting for the small difference noted above. Large incident angles can cause the photon to traverse into the wedge or tower neighboring the seed tower. While the neighboring tower energy is used in the electron energy sum, the neighboring wedge is used in the energy isolation calculation. This causes lower efficiencies than for prompt photons and the total efficiency as a function of incident angle to fall from $\sim$94% to $\sim$80% (see Fig. 5). To take the variation of the efficiency as a function of angle into account it is reasonable to assign a 5% systematic uncertainty to the overall ID efficiency determined for any MC simulation. To study whether any of these ID requirements are overly inefficient by themselves we show distributions and numbers for the fraction of events that pass all but the indicated cut ("(n-1) efficiencies") in Appendix A with the conclusion that we can leave all the requirements unchanged as none of them is overly inefficient. In the next section we will treat the CES χ^2 requirement using a different simulation tool as it is not simulated correctly in *cdfSim*.

Requirement	cumulative # of events		cumulative efficiency (%)		relative efficiency (%)	
	τ_χ =0 ns	τ_χ =10 ns	τ_χ =0 ns	τ_χ =10 ns	τ_χ =0 ns	τ_χ =10 ns
Central ($\lvert\eta\rvert < 1.1$)	101179	90813				
$E_T > 30$ GeV	81730	69788				
$\lvert X_{\text{CES}}\rvert < 21$ cm && 9 cm $< \lvert Z_{CES}\rvert < 230$ cm	64997	44632				
$E_{\text{Had}}/E_{\text{Em}} < 0.125$	64499	44115	99.23±0.03	98.84±0.05	99.23±0.03	98.84±0.05
if $E_T < 20$ GeV then $E^{\text{Iso}}_{0.4\text{ cone}} < 0.1 \cdot E_T$ else $E^{\text{Iso}}_{0.4\text{ cone}} < 2.0 + 0.02 \cdot (E_T - 20)$	63171	42554	97.19±0.06	95.34±0.10	97.94±0.06	96.46±0.09
$N_{\text{trks}} = 0$ or if $N_{\text{trks}} = 1$ then $p_T < 1.0 + 0.005 \cdot E_T$	61629	41963	94.82±0.09	94.02±0.11	97.56±0.06	98.61±0.06
Σp_T of tracks in a 0.4 cone $< 2.0 + 0.005 \cdot E_T$	60820	41392	93.57±0.10	92.74±0.12	98.69±0.05	98.64±0.06
if $E_T < 18$ GeV then $E^{\text{cluster}}_{\text{2nd strip or wire}} < 0.14 \cdot E_T$ else $E^{\text{cluster}}_{\text{2nd strip or wire}} < 2.4 + 0.01 \cdot E_T$	60718	41333	93.42±0.10	92.61±0.12	99.83±0.02	99.86±0.02

TABLE III: The cumulative number of events after each ID cut for the highest E_T CEM photon in the event that comes from a neutralino. Using these numbers we find the corresponding cumulative efficiencies after the fiducial cuts and the relative efficiencies ($N_{\text{pass this cut and all previous}}/N_{\text{pass all previous cuts}}$) with their statistical errors. The distributions are visualized in Fig. 4.

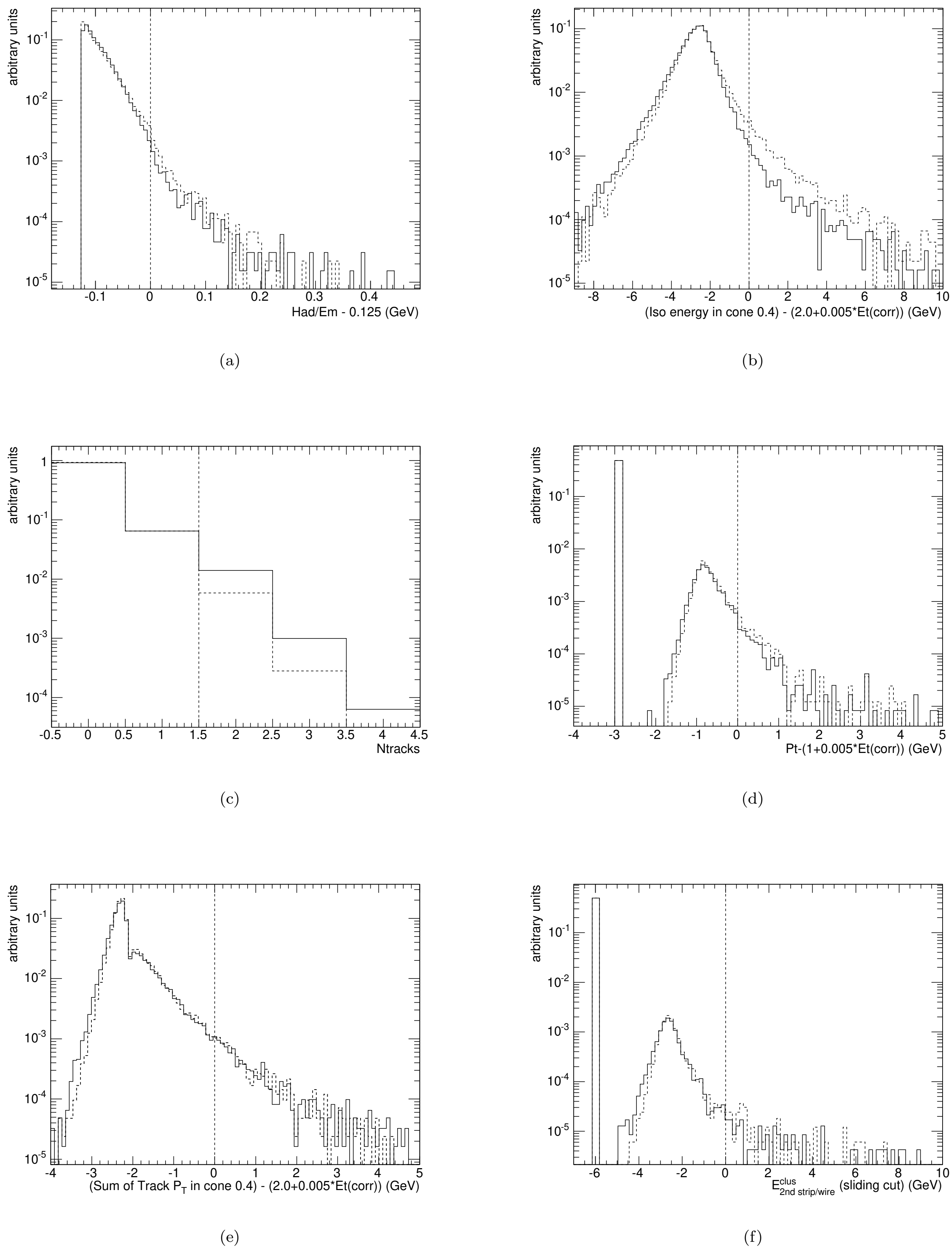

FIG. 4: The normalized ID variable distributions for photons in a GMSB MC with a neutralino of mass 110 GeV produced with *cdfSim*. The plots compare the distributions of prompt photons, simulated as decay photons from neutralinos with a lifetime of 0 ns (solid) to photons from long-lived neutralinos with a lifetime of 10 ns (dashed). A value of <0 means that it passes the corresponding cut. The bin left of the distributions in Fig. (d) collects the photons that have no track associated, in Fig. (f) it shows the photons that have no 2nd cluster. The distributions for all ID variables do not change significantly between the prompt and the long-lived case except for slight deviations in the energy isolation in Fig. (b).

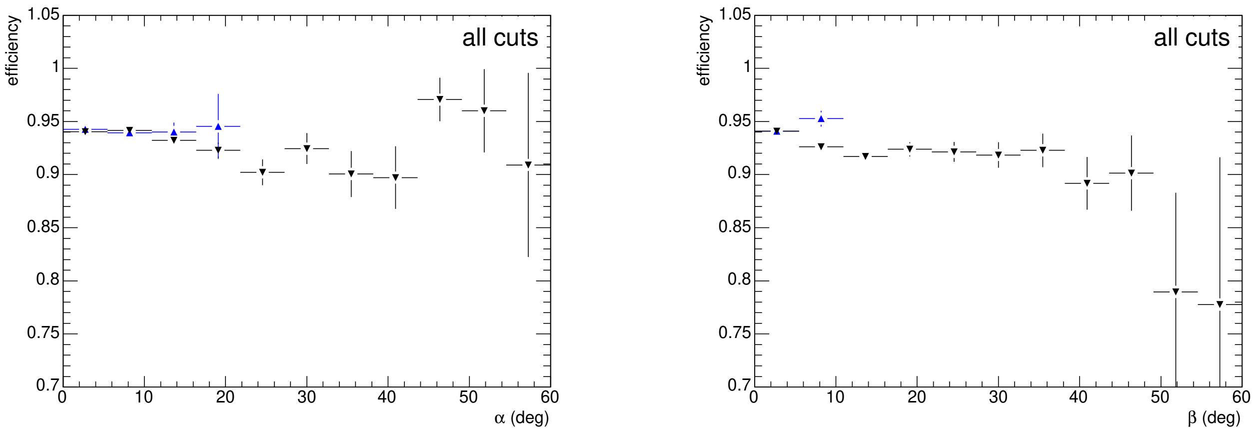

(a)

(b)

FIG. 5: The efficiencies for the standard photon ID requirements (except for the CES-χ^2) for photons in the fiducial portion of the CEM vs. incident angles α and β. We compare the efficiencies from MC using photons in a GMSB model ($m_\chi = 110$ GeV, $\tau_\chi = 10$ ns) (black) with the efficiencies obtained from data using electrons from a $W \rightarrow e\nu$ sample that pass the loose requirements in Table I (blue). The efficiency falls slightly by $\sim 15\%$ from 0 to 60° in β, which mainly comes from the energy isolation. Figures 6 and 7 show the efficiencies for each cut separately.

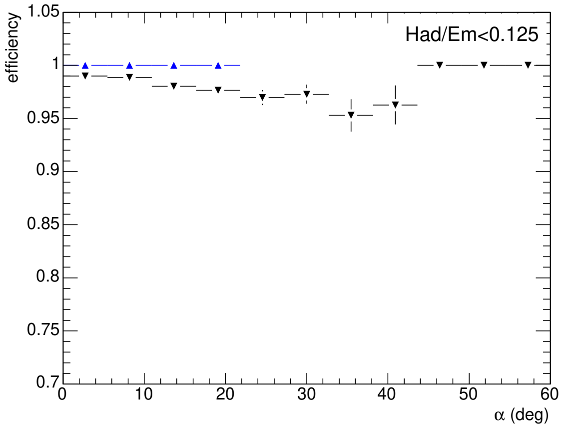

(a)

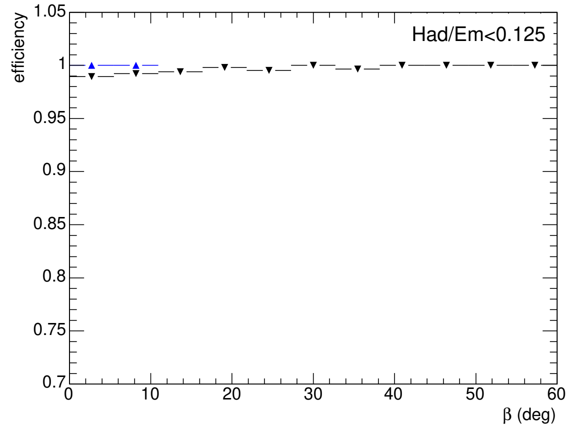

(b)

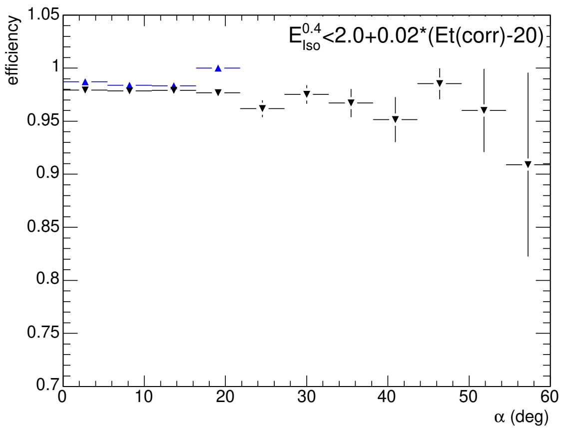

(c)

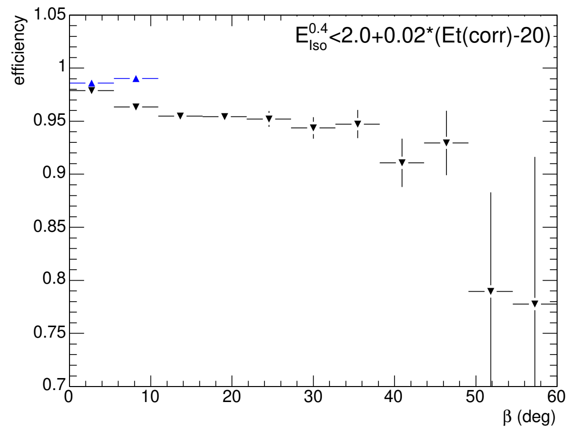

(d)

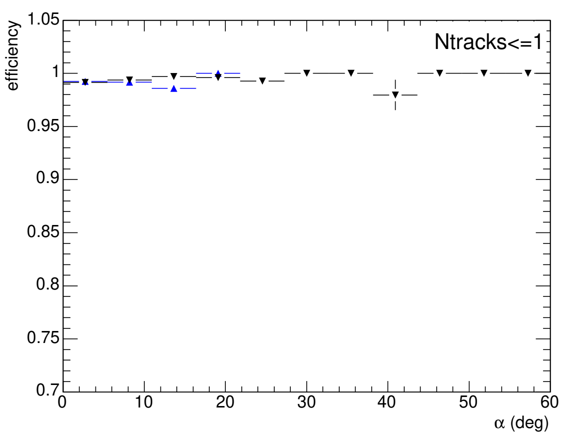

(e)

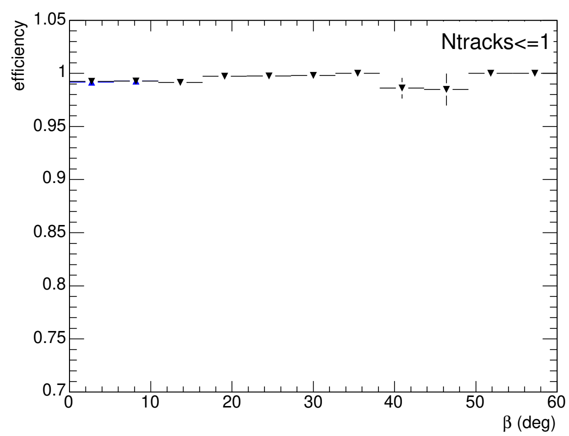

(f)

FIG. 6: The relative efficiencies for each ID variable separately, using the order of the cuts in Table III. The photon MC (reversed triangles) and the electron data sample (upright triangles) match generally well in all shown ID variables in the range for which data is available and are roughly flat except the energy isolation in β (see Fig. (c) and (d)).

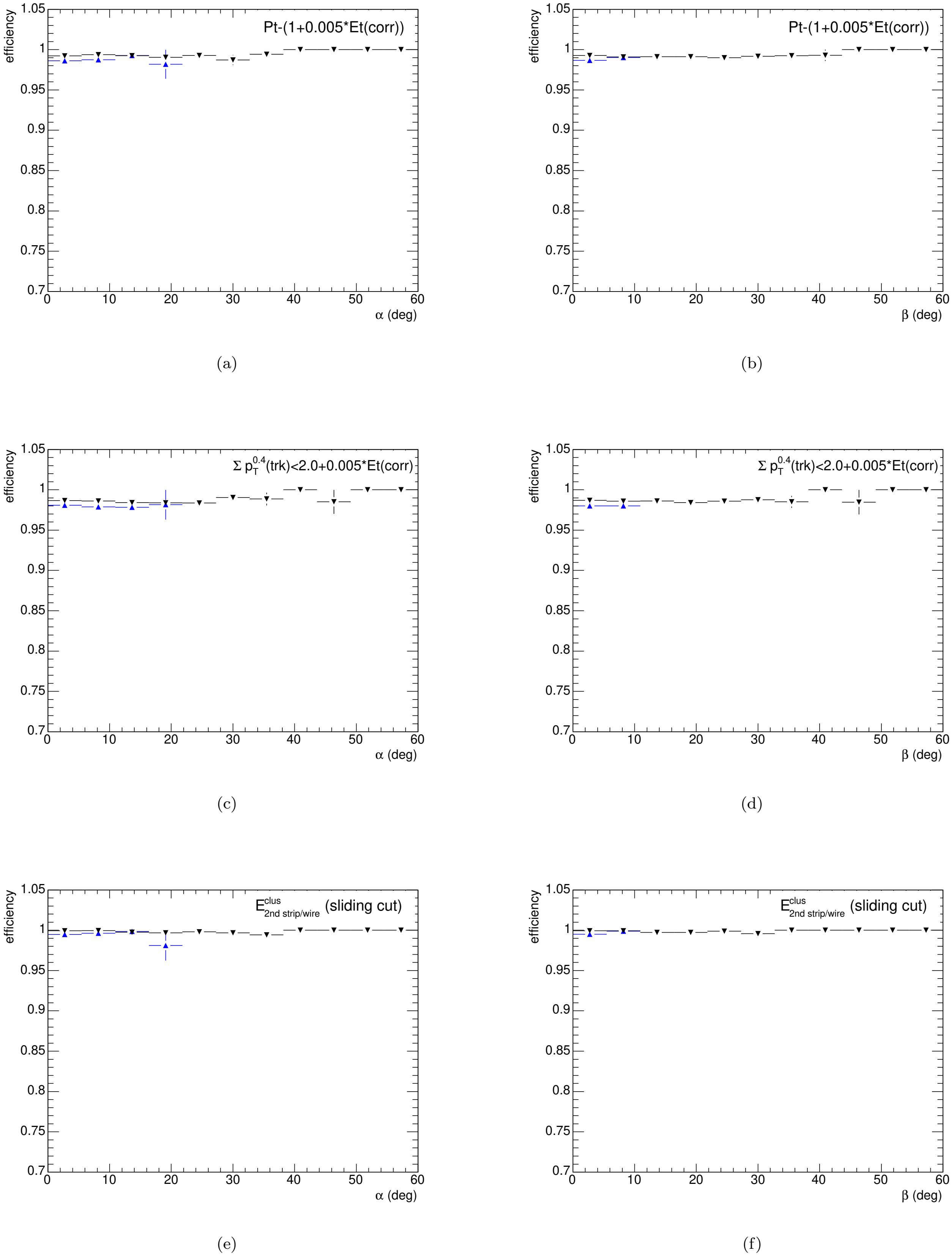

(a) (b) (c) (d) (e) (f)

FIG. 7: A continuation of Fig. 6 for the remaining photon ID variables in Table III.

V. CES-χ^2

This section discusses the CES-χ^2 distribution and the cut efficiency as a function of α and β as simulated using a GEANT simulation of the calorimeter (Geant 3 Wedge Simulation, "G3WS") [7]. The CES contains a strips and a wires subdetector with the strips running in ϕ direction around the detector, and the wires in the z direction. *cdfSim* simulates the CES as follows: it extrapolates the particles produced by its detector simulation from the radius at the coil to the CES according its flight direction. Then it picks the shape from a template that was produced from test beam data based on its z and ϕ position at the CES, independent of its incident angle (see Fig. 10 below). Hence, while the position of the CES cluster is realistic, which is important for the 2nd CES cluster-E_T ID requirement, the shape of the shower in the CES is not reliable for displaced particles. In contrast, G3WS produces the CES shower shape based on the shower produced in the simulated calorimeter. G3WS outputs the energies of all the 128 strips and 64 wires of one half-wedge in ADC counts. Pedestals are simulated using a Gaussian with a mean of 48 ADC counts and RMS of 3.6 (6) for strips (wires) [15] and added to the output energies. The energies are then converted in GeV with the factors 120.0480 for the strips and 240.3846 for the wires [15]. Out of those, 11 strips and 11 wires are selected, each individually centered around the strip and wire respectively with the maximum energy, and given as input to the module *TCesClusterFitter.cc* in Stntuple which does the profile fit and produces an energy-uncorrected χ^2. Lastly, the standard energy correction is performed using *TStntuple::ScaledCesChi2*. Figure 8 compares the normalized CES-χ^2 distributions of 50 GeV photons from G3WS, shot from a fixed vertex into a fixed tower in the CEM (wedge 0, tower 1), and the CES-χ^2 distribution from prompt photons in the *cdfSim* MC. The distributions do not completely match, in particular in the strips as the G3WS yields a worse χ^2 efficiency, as explained below. Figure 9 compares the normalized χ^2 distributions at different incident angles α and β. The shower of a particle that hits the CES at a large α (β) angle appears spread out in z (ϕ) direction due to the projection whereas the shower projection in ϕ (z) remains unaffected, causing only the strips-χ^2 (wires-χ^2) to get large. Figure 9a and b show the χ^2 distribution for strips and wires when the angle α is varied from 0 to 50°. Similarly, varying β between 0 and 60° changes the wire-χ^2 only, whereas the strips remain unchanged (Fig. 9c and d). The individual changes in strips and wires propagate to the total χ^2 in Fig. 9e and f. Figure 10 shows the CES-χ^2 efficiency for the standard photon ID cut $\frac{\chi^2(strips)+\chi^2(wires)}{2}<20$ as a function of α and β of the photon. We note the following (all errors are statistical only):

- Central electron data sample: The incident angle variation is as explained in Section IV. The average efficiency is $(97.8 \pm 0.14)\%$ and shows no angle dependence.

- Central electron *cdfSim* MC sample: Selection and incident angle is treated the same way as the real data sample. The average efficiency is $(99.7 \pm 0.05)\%$ and also shows no angle dependence. From this and the average from the data sample we get the ratio MC/data $= 1.0194 \pm 0.0002$.

- *cdfSim* MC sample with photons from neutralinos with $\tau_{\chi} = 10$ ns: Although the incident angles extend out to $\sim$50° the average efficiency is constant at $(99.5 \pm 0.03)\%$. This is because *cdfSim* picks the shower shape from a template that was produced from test beam data, independent of the incident angle of the photon.

- G3WS: As described above this distribution shows the CES-χ^2 efficiency of photons of energy 50 GeV, shot into the CES at different incident angles. The simulation varies the CES shower shape with incident angle, resulting in a CES-χ^2 efficiency that is flat at low angles, but falls off rapidly at high angles. Using a fit with an error function we find that at low incident angles the average efficiency is $(90.6 \pm 0.8)\%$ for α and $(89.7 \pm 0.7)\%$ for β (from the fit), and does not approach the value from the *cdfSim* MC. The ratio of G3WS to *cdfSim* is 0.911 ± 0.008 and 0.902 ± 0.007 for α and β respectively. This effect is not properly understood [16]. The fit further finds threshold values at 58° and 63° for α and β respectively. While the statistical uncertainty on this fit is small, unfortunately, we do not have a good way of estimating the systematic uncertainties. However, since the distributions in Figure 8 appear to overestimate the width of the χ^2 distribution, there is reason to believe that the threshold values are probably higher than those observed.

In Figure 11 we investigate the possibility of loosening the CES-χ^2 requirement to gain back efficiency or to make the efficiency flat as a function of α and β. For any CES-χ^2 cut we observe a drop in efficiency at a finite angle, so that we do not expect to approach the cut efficiency of prompt photons even if the cut is relaxed.

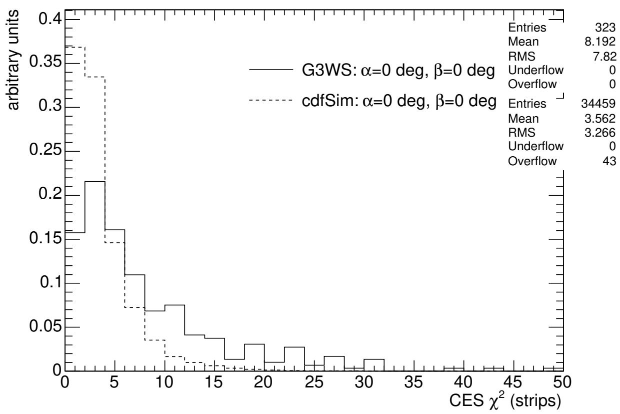

(a)

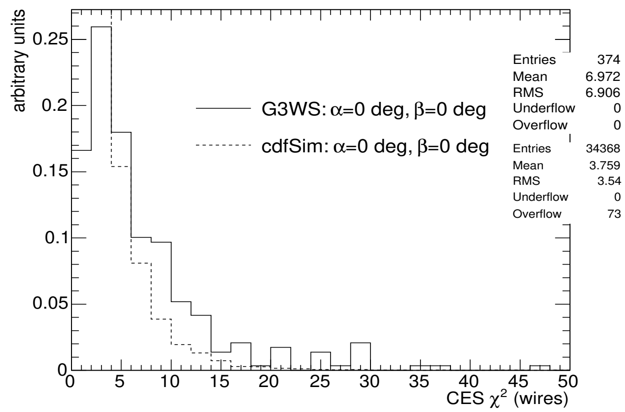

(b)

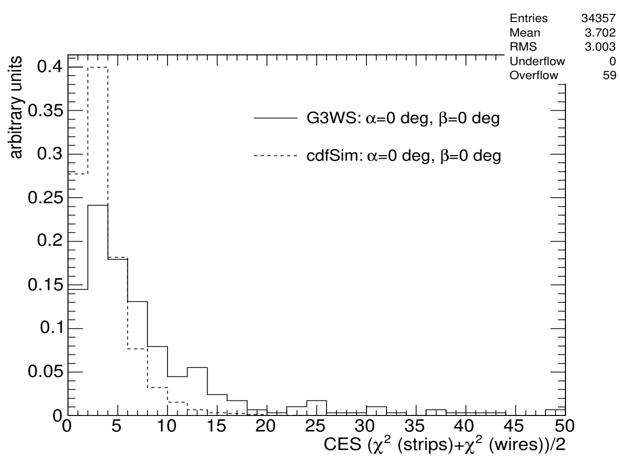

(c)

FIG. 8: A comparison of the CES-χ^2 distributions for a photon of energy 50 GeV that is shot from a fixed vertex into a fixed tower in the CEM (wedge 0, tower 1) at 0° incident angle, simulated with G3WS, and the distribution from the *cdfSim* MC separately for strips (a), wires (b) and combined (c). If simulated correctly, both tools should yield the same distributions, however, there is clearly a mismatch in particular in the strips which leads to a worse combined χ^2 and to a worse χ^2 efficiency for G3WS.

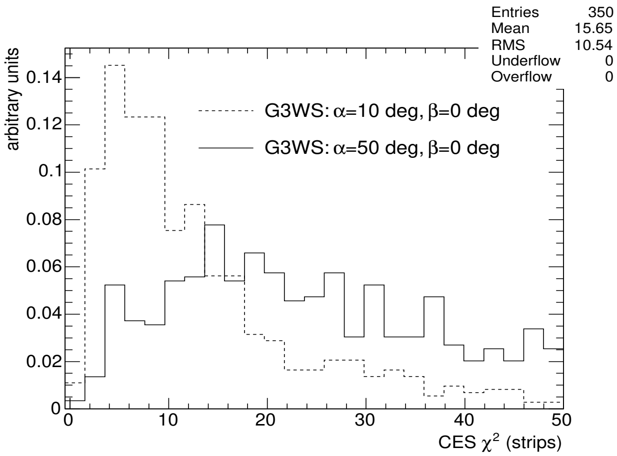

(a)

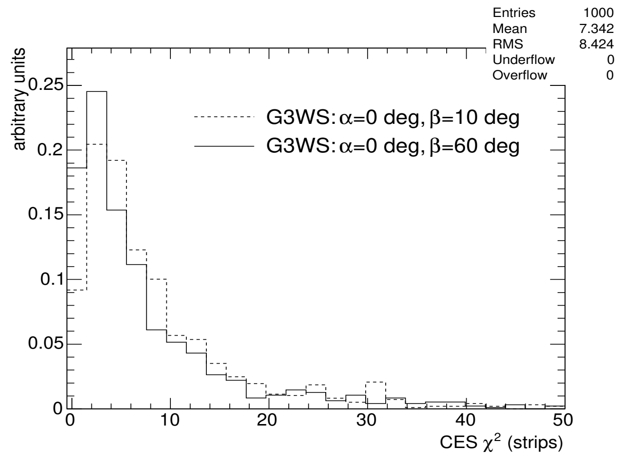

(b)

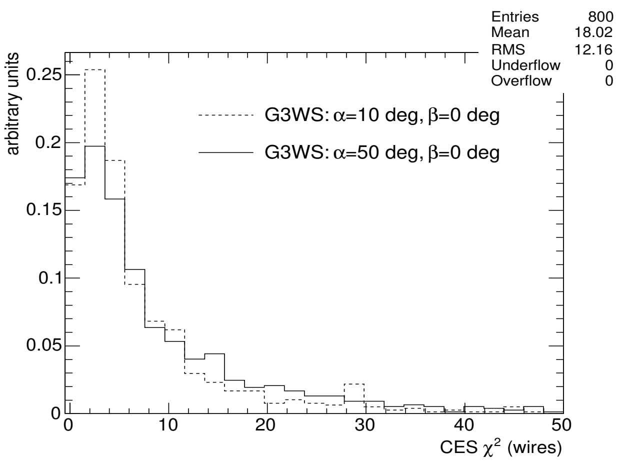

(c)

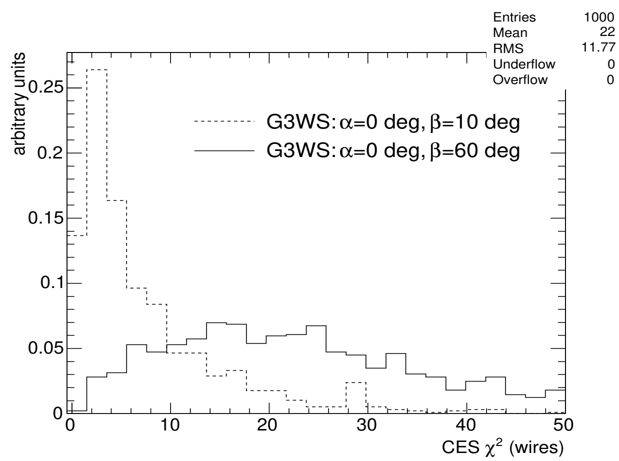

(d)

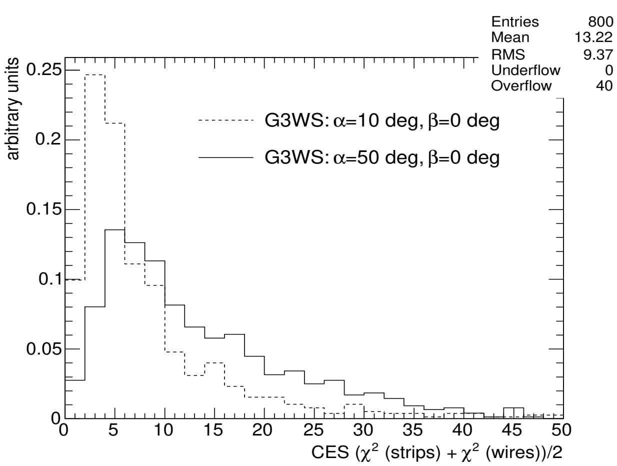

(e)

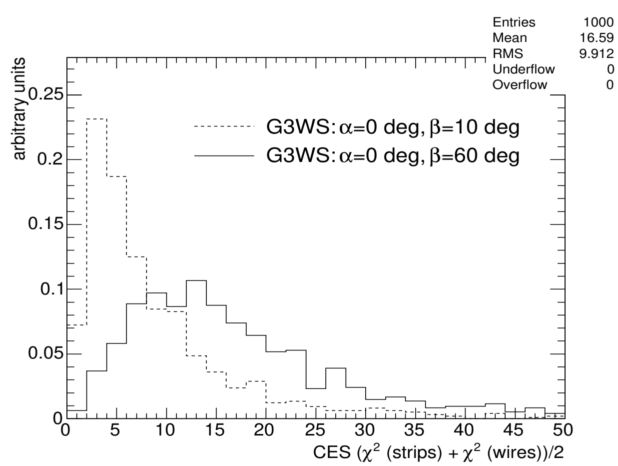

(f)

FIG. 9: The CES-χ^2 distributions for photons simulated with G3WS with the same settings as in Fig. 8, but at different incident angles, simulated with G3WS. The figures in the left column show the distributions in the strips, wires and combined for incident angles of $\alpha = 10^\circ$ (solid) and $\alpha = 50^\circ$ (dashed), with $\beta = 0^\circ$; the figures in the right column for $\beta = 10^\circ$ (solid) to $\beta = 60^\circ$ (dashed), with $\alpha = 0^\circ$. As expected a change of α affects the strips only, a change in β only the wires. Figures (e) and (f) show that the individual effects propagate to the combined CES-χ^2 distribution.

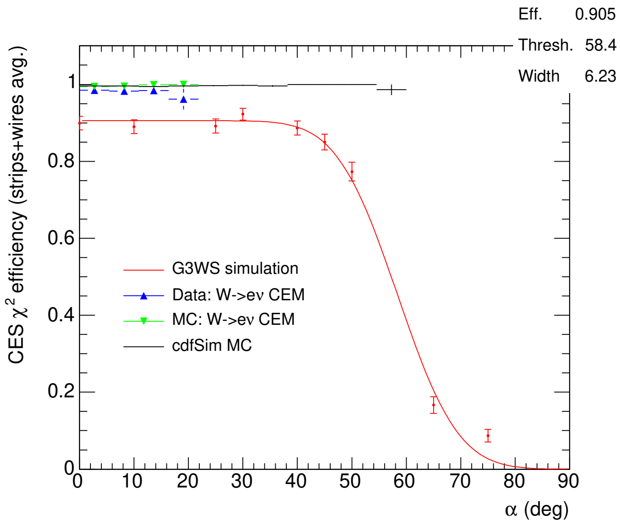

(a)

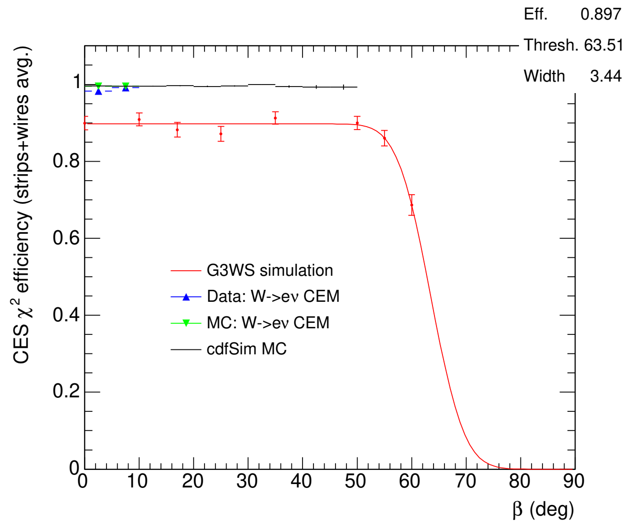

(b)

FIG. 10: A comparison of the CES-χ^2 efficiency as a function of incident angles α and β. We separately plot a $W \to e\nu$ data sample (blue, upright triangles), a $W \to e\nu$ *cdfSim* MC sample (green, inverted triangles) and a GMSB MC sample simulated with *cdfSim* (black), and the efficiency simulated with G3WS, with vertical error bars indicating the statistical error. G3WS, which simulates the angle-dependence of the shower in the CES, shows that the efficiency drops rapidly beyond $\sim$40° for α and $\sim$50° for β respectively. Also shown is a fit to the G3WS points using an error function, with the fit parameters in the upper right box.

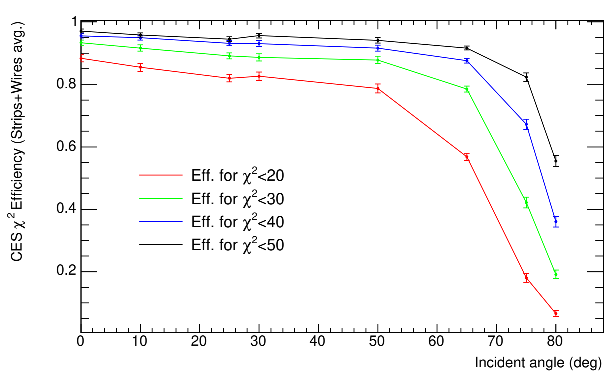

FIG. 11: A comparison of the CES-χ^2 efficiency as a function of incident angle between several χ^2 cuts of 20, 30, 40 and 50, simulated with G3WS. For any cut the efficiency curve turns over at an angle of $\leq$70°.

VI. DISCUSSION

As *cdfSim* and the G3WS simulation disagree in their calculation of the CES-χ^2, and as there is good reason not to trust either of them completely, we have the following options:

(1) We drop the χ^2 requirement. This has the advantage that the requirement no longer produces a loss in efficiency. Also, we would not need to worry about how well the χ^2 is simulated to calculate the efficiency or the systematic error on the efficiency. The drawback is that it would increase the background in searches for new physics; this must be addressed on an analysis-by-analysis basis, but is less of a problem for analyses that require high-E_T photons and dominated by QCD production as the χ^2 variable does not provide strong rejection against π^0 particles at high E_T.

(2) In our acceptance models for simulated events we allow only events that contain photons with incident angles that are well modeled in data (α <18°, β <6°) to contribute. This way our results are robust, but also an underestimate when calculating the acceptance · efficiency and cross section limits for new physics searches. As an example, according to Fig. 3 we would allow $\sim$ 67% ($\sim$ 46%) of signal without (with) a timing requirement with a small systematic error, while assigning a 0% efficiency to the remaining fraction.

(3) We assume the systematic error in the efficiency vs. incident angle distribution from the G3WS simulation is small and calculate the acceptance·efficiency taking into account the variation of the efficiency as a function of incident angles as usual. To do this we would calculate the CES-χ^2 efficiency for each event using the efficiency curves as a function of α and β from Fig. 10, with the indicated efficiency errors, with the incident angle of the GMSB photon on an event-by-event basis. As the result for low incident angles has to coincide with the result from *cdfSim*, we scale the efficiency fit curves to the average data or *cdfSim* efficiency results at angles α <18 and β <6, respectively. The scaled efficiencies as a function of the incident angles are shown with the red (α) and blue (β) curves in Fig. 12. The black dashed line is the integral of the incident angle distribution from Fig. 3, i.e. the acceptance·efficiency if the efficiency were be 1. The black solid line shows the same integral, after weighting each event with the correct efficiency as a function of incident angle. The rightmost value is the resulting CES-χ^2 efficiency of the total sample which is 98.2%. An estimate of the systematic error is 5% but depends critically on the model, in particular on the incident angle distribution, and does not take into account the uncertainty on the threshold in Fig. 10. Since there is reason to believe that the true threshold values are probably larger than those observed this might be a safe assumption.

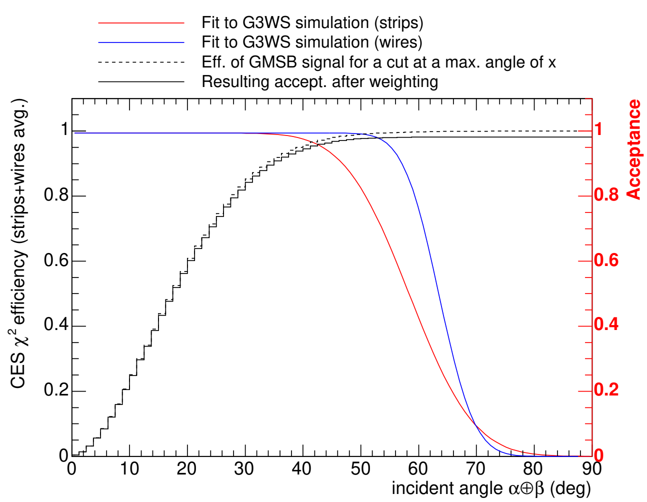

FIG. 12: The acceptance we would get if we only allowed events with the angle shown on the x-axis or less to contribute. The black solid histogram shows the fraction from the GMSB signal only and the black dashed histogram shows the fraction of photons after taking into account the χ^2 efficiency from the fit as a function of α and β separately from G3WS which is shown with the red and the blue functions. All distributions are scaled to the *cdfSim* MC efficiency of 99.4%.

VII. CONCLUSION

We have studied the photon ID variable distributions and the efficiencies for the standard ID cuts for for photons from long-lived, heavy neutral particles as can be found in GMSB models. As *cdfSim* models the data well at low angles and we find that the ID efficiencies are largely unchanged as a function of the photon incident angle, with the small exception of the energy isolation, which we believe can be used as is. We believe a systematic uncertainty of 5% easily covers the variation for all but the most pathological models. However, there is no reason to believe that *cdfSim* simulates the CES-χ^2 distribution and efficiency correctly. An alternative simulation, G3WS, developed to simulate the shower in the CES correctly shows a sharp efficiency drop at around 50-60° in α and β. However, this simulation is not completely understood as it gets the low angle efficiency wrong, and suggests that we should not use it as an efficiency estimate either. While we have presented criteria to help a prospective analysis decide whether to drop the requirement and how to estimate the efficiency·acceptance, the final decision is very analysis dependent as other considerations have to be taken into account as e.g. the size of the background when the cut is dropped.

Acknowledgments

The authors would like to thank R. Blair and R. Culbertson for providing the necessary Monte Carlo tools and for helpful suggestions.

[1] http://hepr8.physics.tamu.edu/hep/emtiming/
[2] H Frisch, H. Sanders, M. Cordelli, F. Happacher, S. Miscetti, R. Wagner, M. Goncharov, T. Kamon, V. Khotilovich, V. Krutelyov, S.W. Lee, D. Toback and P. Wagner, "The Timing System for the CDF Electromagnetic Calorimeters," CDF Note 7918 (2005).
[3] P. Wagner and D. A. Toback, Phys. Rev. D **70**, 114032 (2004).
[4] See for example S. Ambrosanio, G. L. Kane, G. D. Kribs, S. P. Martin and S. Mrenna, Phys. Rev. D **54**, 5395 (1996) or C. H. Chen and J. F. Gunion, Phys. Rev. D **58**, 075005 (1998).
[5] Photons from cosmic rays hit the detector in a large incident angle as well, however as we do not know their "vertex," i.e. their incident angle event by event, we have to use a MC.
[6] Photon webpage of CDF: http://www-cdf.fnal.gov/internal/physics/photon/docs/cuts.html
[7] R. Blair, "A Geant Simulation of the CES," CDF Note 1436 (1991).
[8] PYTHIA: T. Sjöstrand, L. Lönnblad and S. Mrenna, arXiv:hep-ph/0108264; cdfSim: "Tutorial on cdfSim," G.S. Sganos.
[9] B. C. Allanach *et. al.*, Eur. Phys. J. C**25**, 113 (2002). We take SPS 8.
[10] M. Goncharov, V. Krutelyov, D. Toback and P. Wagner, "Space-Time Vertex Reconstruction Using COT Tracks," CDF Note 8015 (2005).
[11] M. Goncharov, V. Krutelyov, D. Toback and P. Wagner, "Search for Neutral, Long-Lived Particles that Decay to Photons," CDF Note 8016 (2005).
[12] M. Goncharov, V. Krutelyov, D. Toback and P. Wagner, "Resolution and Simulation of the EMTiming System," CDF Note 7928 (2006).
[13] The requirement on the corrected arrival time of the photon will most probably be imposed in an analysis of a search for long-lived particles as in Ref. [11].
[14] Note that while α varies for the prompt electrons with the vertex position as described in Section III, we estimate the efficiency as a function of β by varying the CES X of the electron, assuming that a large CES X is equivalent of a large β. This allows for a maximum angle of $\sim 6^\circ \approx$ arctan(20cm/183cm) where 20 cm is the half-width of a CEM tower.
[15] http://www-cdf.fnal.gov/internal/physics/photon/docs/CES_CPR_geometry.html
[16] The hypothesis has always been that GEANT3 does not properly model the keV level phenomenon which are important to gas detectors. Cutoffs and cross sections were tuned for higher density ionization devices/detectors. This, however, is just a hypothesis. The standard simulation on the other hand, which is based on test beam data, has some canned way to deal with z variation, but no way at all to deal with showers from things that originate from $(x, y) \neq (0, 0)$ and even the z variation is probably limited. The only thing it includes is the type of effect described in CDF note 1329 and these are not meant to cover large variations in the origin. (priv. comm. with B. Blair)

APPENDIX A: (N-1) EFFICIENCIES

In this section we show the (n-1) efficiencies for the various ID requirements. The (n-1) efficiency is defined as the number of events that pass all requirements divided by the events that pass all cuts with no requirement on this cut. Figures 13 and 14 show the ID efficiencies as a function of angles α and β and Table IV summarizes the numbers. None of the listed cuts is overly inefficient, which is why we decided not to remove any of the ID requirements for CDF note 8016 [11].

Requirement	(n-1) efficiency (%)	
	τ_{χ} =0 ns	τ_{χ} =10 ns
Central ($\|\eta\| < 1.1$)	1	1
$E_T > 30$ GeV	88.4±0.3	85.9±0.1
$\|X_{\rm CES}\| < 21$ cm && 9 cm $< \|Z_{CES}\| < 230$ cm	85.8±0.36	79.8±0.17
$E_{\rm Had}/E_{\rm Em} < 0.125$	99.5±0.08	99.0±0.05
if $E_T < 20$ GeV then $E^{\rm Iso}_{0.4\ \rm cone} < 0.1 \cdot E_T$ else $E^{\rm Iso}_{0.4\ \rm cone} < 2.0 + 0.02 \cdot (E_T - 20)$	98.5±0.13	97.6±0.07
$N_{\rm trks} = 0$ or if $N_{\rm trks} \geq 1$ then $p_T < 1.0 + 0.005 \cdot E_T$	99.2±0.10	99.3±0.04
Σp_T of tracks in a 0.4 cone $< 2.0 + 0.005 \cdot E_T$	98.0±0.15	97.9±0.07
if $E_T < 18$ GeV then $E^{\rm cluster}_{\rm 2nd\ strip\ or\ wire} < 0.14 \cdot E_T$ else $E^{\rm cluster}_{\rm 2nd\ strip\ or\ wire} < 2.4 + 0.01 \cdot E_T$	99.9±0.04	99.8±0.02

TABLE IV: The (n-1) efficiencies for prompt photons and photons from neutralinos with τ_{χ} = 10 ns. The (n-1) efficiency is defined as the fraction of events that pass all but this cut, with their statistical errors for the highest E_T CEM photon in the event. The distributions as a function of incident angles α and β are visualized in Figs. 13 and 14.

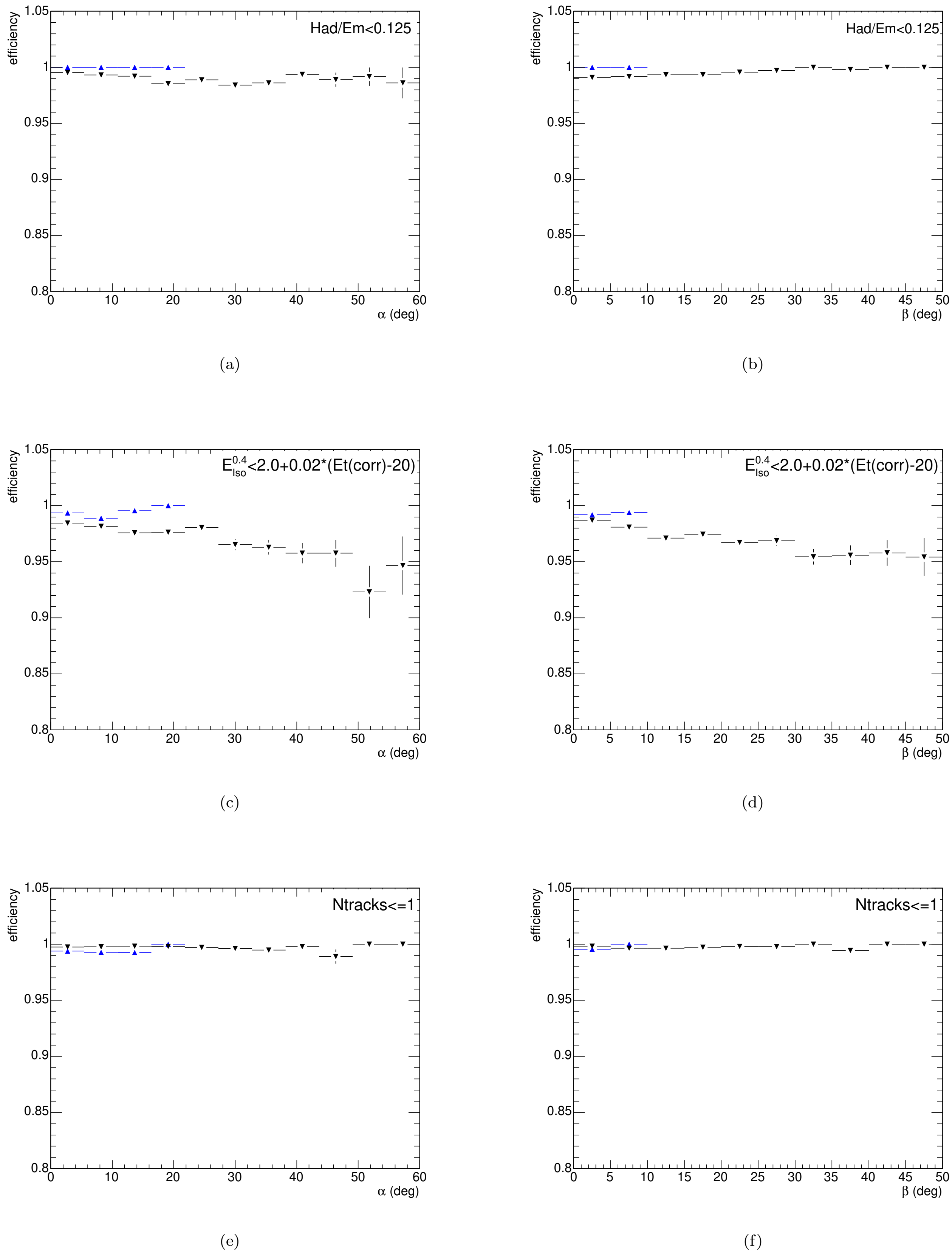

FIG. 13: The (n-1) efficiencies for each ID variable for photons in the fiducial portion of the CEM vs. incident angles α and β. We compare the efficiencies from MC using photons in a GMSB model ($m_\chi = 110$ GeV, $\tau_\chi = 10$ ns) (black) with the efficiencies obtained from data using electrons from a $W \rightarrow e\nu$ sample that pass the loose requirements in Table I (blue). The photon MC and the electron data sample match generally well in all shown ID variables in the range in which data is available except the energy isolation (see Fig. (c) and (d)).

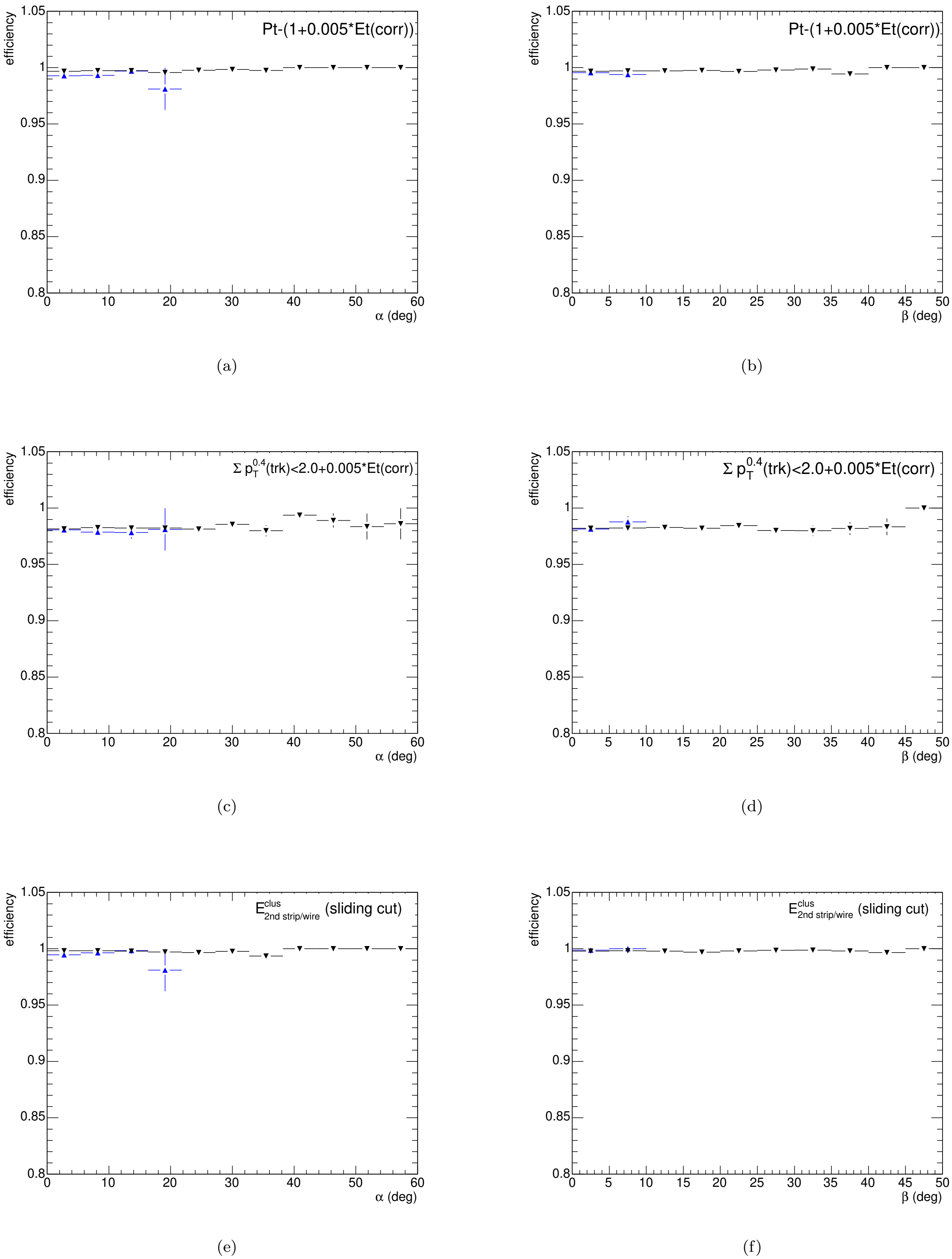

FIG. 14: These plots continue the (n-1) efficiencies of photon ID variables (see Table IV) vs. incident angles α and β from Fig. 13.